ACS OMEGA

Open Access

http://pubs.acs.org/journal/acsodf

Article

Highly Efficient Recovery of Au(I) from Gold Leaching Solution Using Sodium Dimethyldithiocarbamate

Peng Yang, Xinrong Li, Shuliang Chen, Futing Zi, and Xianzhi Hu*

Cite This: *ACS Omega* 2024, 9, 20547−20556

Read Online

ABSTRACT: As a sustainable, nontoxic and environmentally friendly cyanide-free gold leaching agent, thiosulfate has been applied to some extent in the field of hydrometallurgy. However, the difficult recovery of gold ions in gold leaching solutions limits further application of thiosulfate gold leaching technology. This study demonstrated the feasibility of gold recovery by sodium dimethyldithiocarbamate (SDD) precipitation and recycling of ammonia and a lixiviant in solution. SDD achieved the purpose of recovering gold by forming granular precipitates with gold ions in solution. It can almost completely recover gold ions in 2.5−17.34 mg/L of gold leaching solution within 1 min at 25 °C, in which a gold recovery capacity of 7.99 kg/t is achieved. The leaching rate of gold ore did not change significantly after recycling the residual ammonia and thiosulfate in the leaching solution after gold recovery by SDD, and its leaching rate basically remained at 81%. The mechanism of SDD recovering Au was determined to involve the ligand exchange of SDD^- and $Au[(S_2O_3)_2]^{3-}$. Moreover, the interaction mechanism between SDD and Au(I) was further validated by density functional theory calculations. Considering its low cost, simple technology, and environmental friendliness, the SDD precipitation process has the potential for large-scale application in gold recovery from thiosulfate gold leaching solutions.

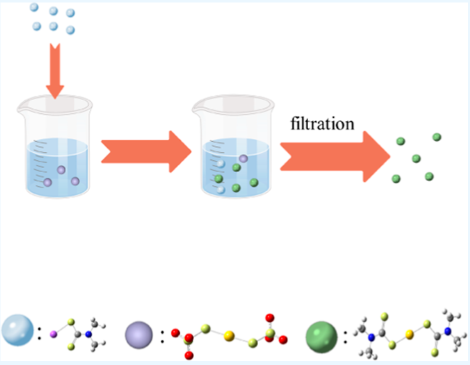

1. INTRODUCTION

Cyaniding is a very effective method of gold extraction in the field of hydrometallurgy. However, cyanide has been banned by many countries and regions due to its dramatic toxicity.[1] At present, the more common noncyanide gold leaching reagents include thiourea, halogens, thiocyanate, thiosulfate, and so on.[2−5] Among these reagents, thiosulfate has become the most promising noncyanide lixiviant because of its nontoxic property, environmental protection, and low corrosion.[3,4] In addition, carbonaceous or copper-bearing gold ores that cannot be treated by cyanidation can also be processed effectively by thiosulfate.[3,5] In particular, when a copper−ammonia complex was added to the solution as catalytic oxidant, a satisfactory gold leaching effect could be processed in a short time,[6] the mechanism of which is shown in eq 1. However, the industrial application of this process is limited due to the difficulty in recovering gold.[7−9]

$$Au + 5S_2O_3{}^{2-} + Cu(NH3)_4^{2+} \rightarrow Au(S_2O_3)_2^{3-} + 4NH_3 + Cu(S_2O_3)_3^{5-} \quad (1)$$

In view of the difficulty of gold recovery in the thiosulfate leaching solution, the three existing methods for recovering gold(I) mainly include solvent extraction, metal replacement, and adsorption.[6,8] KeJun used trioctylmethylammonium chloride to extract Au(I) from thiosulfate solution, and its recovery efficiency reached 99%;[10] Harshit Mahandra used phosphine ionic liquids to recover gold from thiosulfate solutions with a gold ion recovery efficiency of 98%.[2] However, the residual extractant and organic phase in the leaching solution were not conducive to the recycling of ammonia and the lixiviant, resulting in increased costs and serious ammonia pollution; furthermore, the excessive use of organic reagents has also caused environmental pollution.[4] It was feasible to recover Au(I) from thiosulfate solution using base metals such as copper, zinc, and aluminum as replacement reagents.[11] However, the replacement reaction introduced the ions of the reducing reagent into the leaching solution, resulting in the accumulation of reagent ions in the solution, making it difficult to recycle the ammonia and lixiviant; in particular, the decomposed products of thiosulfate are likely to form a passivation film on the surface of the base metal, which hinders the progress of the replacement reaction, thereby increasing the consumption of the base metal and increasing the cost. Yu and Chen et al. obtained a superior effect of recovering Au(I) in thiosulfate solution by using modified activated carbon and silica gel.[6,12] However, in the experiments, it was found that the

Received: February 28, 2024
Revised: April 15, 2024
Accepted: April 18, 2024
Published: April 26, 2024

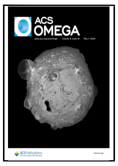

https://doi.org/10.1021/acsomega.4c01941

Table 1. Elemental Analysis Results of Gold Oxide

elements	O	Na	Mg	Al	Si	P	S	K	Ca	Ti	Fe	Mn	Cu
content (%)	36.71	1.08	2.34	7.86	24.97	0.12	1.22	2.24	5.74	0.77	5.17	0.12	0.05

recovery effect of the modified activated carbon and silica gel on gold ions was limited in the leaching solution rich in impurity ions; in particular, two steps of adsorption and desorption are required to enrich gold in solution by adsorption, which is complicated and uneconomical.[13] In addition to the above three methods, an in situ reduction method for Au(I) recovery by MoS_2 was proposed recently. Although this method can directly obtain Au(0),[13,14] it is not feasible in the gold leaching solution with low concentrations. Therefore, this study developed a new process of recovering Au(I) that is simpler, has high efficiency, and lower-cost than the above recovery methods and can not only completely recover the low and high concentrations of gold in the leaching solution in one step but also realize the recycling of ammonia and the lixiviant in the solution.

Sodium dimethyl dithiocarbamate (SDD) is a cheap and readily available organic sulfide, which dissolves in alkaline solutions to form an S-containing anionic group $(CH_3)_2NCSS^-$ (SDD^-), which can coordinate around transition metals strongly to generate insoluble complexes due to intra ligand $\pi-\pi^*$ transitions associated with N−C−S and S−C=S.[15] Furthermore, based on the hard and soft acids and bases (HSAB) fundamental theory, S^- is a soft base with a large size and low electronegativity that interacts strongly with many soft acids such as Pt(II) and Hg(II);[6] gold exists in the form of $Au[(S_2O_3)_2]^{3-}$ in the thiosulfate leaching solution, which is a soft acid. Therefore, SDD can be used as a chelating precipitant to recover Au(I) from a gold leaching solution.

Here, it was found that SDD can achieve the purpose of gold ion enrichment by forming granular precipitations with Au(I) in the thiosulfate leaching solution and the recycling of thiosulfate and ammonia in the solution. To study the recovery performance of SDD for Au(I), the SDD dosage, reaction time, reaction temperature, gold concentration, and recycling performance of thiosulfate and ammonia in the gold leaching solution after recovering Au(I) were investigated. The reaction mechanism of SDD and Au(I) was further explored by Fourier transform infrared spectroscopy (FT-IR) and X-ray photoelectron spectroscopy (XPS). Furthermore, the mechanism of SDD-Au formation was further investigated by using density functional theory.

2. MATERIALS AND METHODS

2.1. Materials. SDD was purchased from the McLean's reagent web site. All conventional chemical reagents used in this study, such as ammonia solution (NH_3, 28%), sodium thiosulfate ($Na_2S_2O_3$), hydrogen peroxide (H_2O_2, 30%), and copper sulfate pentahydrate ($CuSO_4·5H_2O$), were of analytical reagent grade. $Au[(S_2O_3)_2]^{3-}$ solution was configured using gold powder (99.99%) from Sino-Platinum Metals Corporation, China.

2.2. Methods. *2.2.1. Preparation of Pure $Au[(S_2O_3)_2]^{3-}$ Solution.* $Au[(S_2O_3)_2]^{3-}$ solution was prepared according to the method of Wang et al.,[3] and pH of the solution was adjusted by HCl and NaOH. First, the gold powder with a purity of 99.99% was added to a beaker containing aqua regia with a volume ratio of 1:1 and heated for dissolution. Next, few drops of 10% KCl were added to the beaker. Finally, a pure $Au[(S_2O_3)_2]^{3-}$ solution was obtained by adding the sodium thiosulfate solution of determined concentration to the beaker after drying.

2.2.2. Preparation of Cu^{2+}-NH_3 Solution. The molar ratio of NH_3 and Cu^{2+} used in this experiment was 80:1. First, a certain amount of ammonia solution was added to a beaker containing water. Then, a Cu^{2+}-NH_3 solution was obtained by adding copper(II) sulfate pentahydrate solution of defined concentration to the above beaker and rapid stirring.

2.2.3. Preparation of Thiosulfate Gold Leaching Solution. To begin, gold ore extracted from the mine was directly pulverized into a fine powder using a ball mill. Subsequently, the powder was screened with 200 mesh to obtain pretreated gold ore with a gold content of 8.32 kg/t. The specific contents of other elements in the gold ore are shown in Table 1.[16] The pretreated 150 g of gold ore was placed in a 250 mL Erlenmeyer flask with 100 mL of Cu^{2+}-NH_3 solution. Then, 0.1 mol sodium thiosulfate was added to the Erlenmeyer flask.[7,14] Next, the Erlenmeyer flask was placed in a constant temperature water bath set to 25 °C and leached with a mechanical stirrer at 350 rpm for 24 h. Finally, the leached ore pulp was filtered to obtain a thiosulfate gold leaching solution. The gold leaching rate of the gold ore was 83.35% after atomic absorption spectroscopy (AAS) determination. In addition, after the end of gold leaching, thiosulfate was basically consumed, and its specific consumption was 87%.

2.2.4. Recovery Test. To study the recovery effect of SDD for Au(I) in solution, a certain concentration of 100 mL of thiosulfate gold leaching solution and a certain amount of SDD were placed in a 250 mL Erlenmeyer flask. Then, the mixture was placed in a water bath at a certain temperature with a mechanical stirrer at 200 rpm for a period of time. Finally, the gold-containing precipitate obtained after filtration was collected. The specific test process is shown in Figure 1. The change of gold ion concentration in the solution before and after the reaction was analyzed by an atomic absorption spectrometer. The recovery capacity, Q (mg/g), and the recovery efficiency, R (%), were calculated using eqs 2 and 3, respectively.

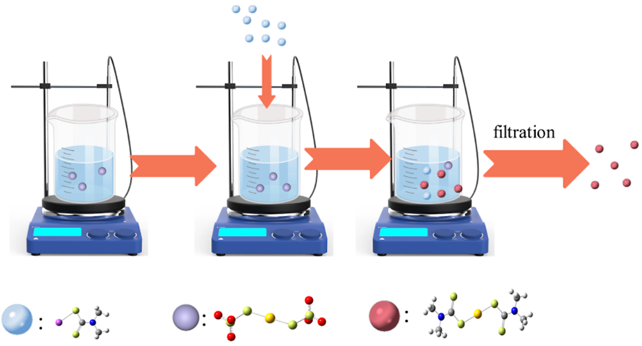

Figure 1. Specific process of SDD recovery of gold(I).

$$Q = \frac{C_0V_0 - C_tV_t}{m} \tag{2}$$

$$R = \frac{C_0V_0 - C_tV_t}{C_0V_0} \times 100\% \tag{3}$$

herein, C_0 and C_t are the concentrations of thiosulfate solution containing Au(I) ions before and after the reaction, respectively. V_0 and V_t are the volumes of solution containing Au(I) ions before and after the reaction. In subsequent experiments, the product of the reaction between SDD and Au(I) was named SDD-Au.

2.2.5. Material Characterization. The changes in gold concentration in solution before and after the reaction were analyzed by AAS (AAS-300, PerkinElmer, USA). The content of the main elements in gold ore was determined by X-ray fluorescence (Malvern Panalytical). The chemical environment of elements in SDD and SDD-Au were characterized by XPS (PHI5000, ULVAC-PHI, Japan). The surface morphologies and elemental compositions of SDD and SDD-Au were determined by scanning electron microscopy-energy dispersive X-ray spectroscopy (SEM-EDS) (Phenom Prox, FEI Co). At the same time, the functional groups of these substances were also studied by FT-IR (Nicolet iS10, Thermo Fisher). In addition, the stabilities of SDD and SDD-Au were also investigated by thermogravimetric analysis (TGA) (PerkinElmer TGA-8000).

3. RESULTS AND DISCUSSION

3.1. Material Characterization. *3.1.1. FT-IR Results.* FT-IR spectroscopy was used to detect the functional groups of SDD and SDD-Au to explore the reaction mechanism between SDD and Au, where SDD-Au precipitated after the reaction between SDD and pure $Au[(S_2O_3)_2]^{3-}$ solution. The results are illustrated in Figure 2. In the FT-IR spectrum of SDD, the absorption peak at 2924 cm^{-1} is ascribed to the C−H vibration.[17] The absorption band at 962 cm^{-1} is related to the C−S vibration,[18,19] whereas the absorption peaks at 1043 and 1117 cm^{-1} are attributed to the C═S vibration.[19,20] The absorption band at 1487 cm^{-1} is ascribed to the C−N of the −N−CSS vibration.[21] In the case of SDD-Au, it can be found that all peak intensities are significantly lower than those for SDD. Compared with SDD, the absorption band of the C−S functional group on SDD-Au changed to 985 cm^{-1}, indicating that the S in C−S group coordinated with Au(I) in the reaction process.[22] The absorption bands of the C═S functional group on SDD-Au changed to 1053 and 1139 cm^{-1}; these blue-shifts indicate the presence of charge transfer in the C═S group.[23] Moreover, the differences between the SDD and SDD-Au also appear in the C−N of −N−CSS, and slight shifting of the C−N bands to a higher wavenumber (1487−1500 cm^{-1}) indicates the partial double bond between N and C atoms of the N−CSS group in SDD-Au.[24]

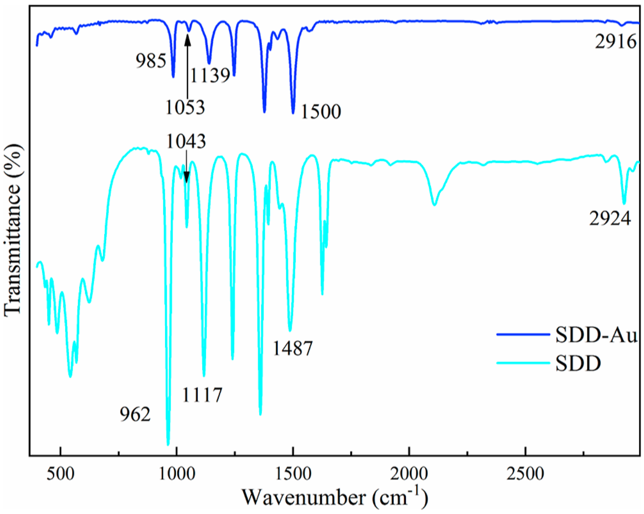

Figure 2. FT-IR spectra of SDD and SDD-Au.

3.1.2. XPS Results. To determine the mechanism of action of SDD and Au, XPS was used to determine the chemical environment of elements in SDD and SDD-Au; the results are shown in Figure 3. To more clearly determine the action mode of SDD and Au(I), SDD-Au was the precipitation after the reaction between SDD and pure $Au[(S_2O_3)_2]^{3-}$ solution. As seen in Figure 3a, a strong characteristic peak of Au is observed in the spectrum of SDD-Au, indicating that gold ions in the solution were recovered by forming precipitates with SDD. Furthermore, the S 2p peak of $S_2O_3{}^{2-}$ is not observed at a binding energy of 167.7 eV, which indicates that the obtained gold-containing precipitation had no $S_2O_3{}^{2-}$ ions present.[25] The high-resolution spectrum of SDD-Au (Figure 3h) shows that the binding energies of Au $4f_{7/2}$ and $4f_{5/2}$ are 85.03 and 88.70 eV, respectively, indicating that the gold here exists in the +1 oxidation state.[26]

The C 1s XPS spectra of SDD and SDD-Au are shown in Figure 3b,c. It can be found that there is an identical peak at 284.80 eV in the C 1s spectra of both samples, which is ascribed to the introduction of a new contaminating carbon source into the sample surface in the process of testing. In Figure 3b, the peak at 285.42 eV can be assigned to the binding energy of C 1s on $-N-(CH_3)_2$;[27] the peak at 288.53 eV can be attributed to the binding energy of C 1s on −N−CSS−.[28] In Figure 3c, it can be found that the binding energy of C 1s on $-N-(CH_3)_2$ changed from 285.42 to 285.91 eV, and the binding energy of C 1s on −N−CSS− changed from 288.53 to 287.20 eV after SDD and Au(I) formed a chelating precipitation, indicating that there is a charge transfer between the carbon atoms in the $-N-CH_3$ and −N−CSS− groups and the surrounding adjacent atoms.[29] In Figure 3d, the peak at 399.69 eV can be ascribed to the binding energy of N 1s on $-SSC-N-CH_3$.[30] However, it can be seen from Figure 3e that the chemical environment of N in the precipitated SDD-Au has changed, and its binding energy has increased by 0.72 eV, which indicates that the chemical environment of N has changed. The change of the chemical environment of N element in SDD-Au is consistent with the conclusion that a partial double bond exists between the N and C atoms of the N−CSS group in SDD-Au in the FT-IR characterization. In Figure 3f, the peaks at 161.58 and 161.85 eV can be ascribed to the binding energy of S $2p_{3/2}$ in C═S and C−S, respectively;[30,31] the peak at 167.90 eV can be assigned to the binding energy of S═O because parts of the C−S groups are oxidized to sulfonic acid groups.[7,32] It can be found that the difference in binding energy between the two sulfur elements in the −CSS− functional group is not large, which may be due to the coexistence of C═S and C−S groups, resulting in changes in the chemical bonds between them. In Figure 3g, it can be found that, compared with SDD, the chemical environment of S on SDD-Au has changed, and the binding energies of S 2p3/2 in C═S and C−S are increased by 1.21 and 1.30 eV, respectively. Clearly, the chemical environment of the C═S and C−S functional groups changed upon the formation of the precipitate. In addition, the binding energy of the sulfonic acid group in SDD-Au disappears, indicating that SDD can react with Au to form a precipitate only when the C−S bond exists.

Therefore, combining the FT-IR and XPS results, it can be speculated that the formation of the SDD-Au chelating complex

https://doi.org/10.1021/acsomega.4c01941
ACS Omega 2024, 9, 20547−20556

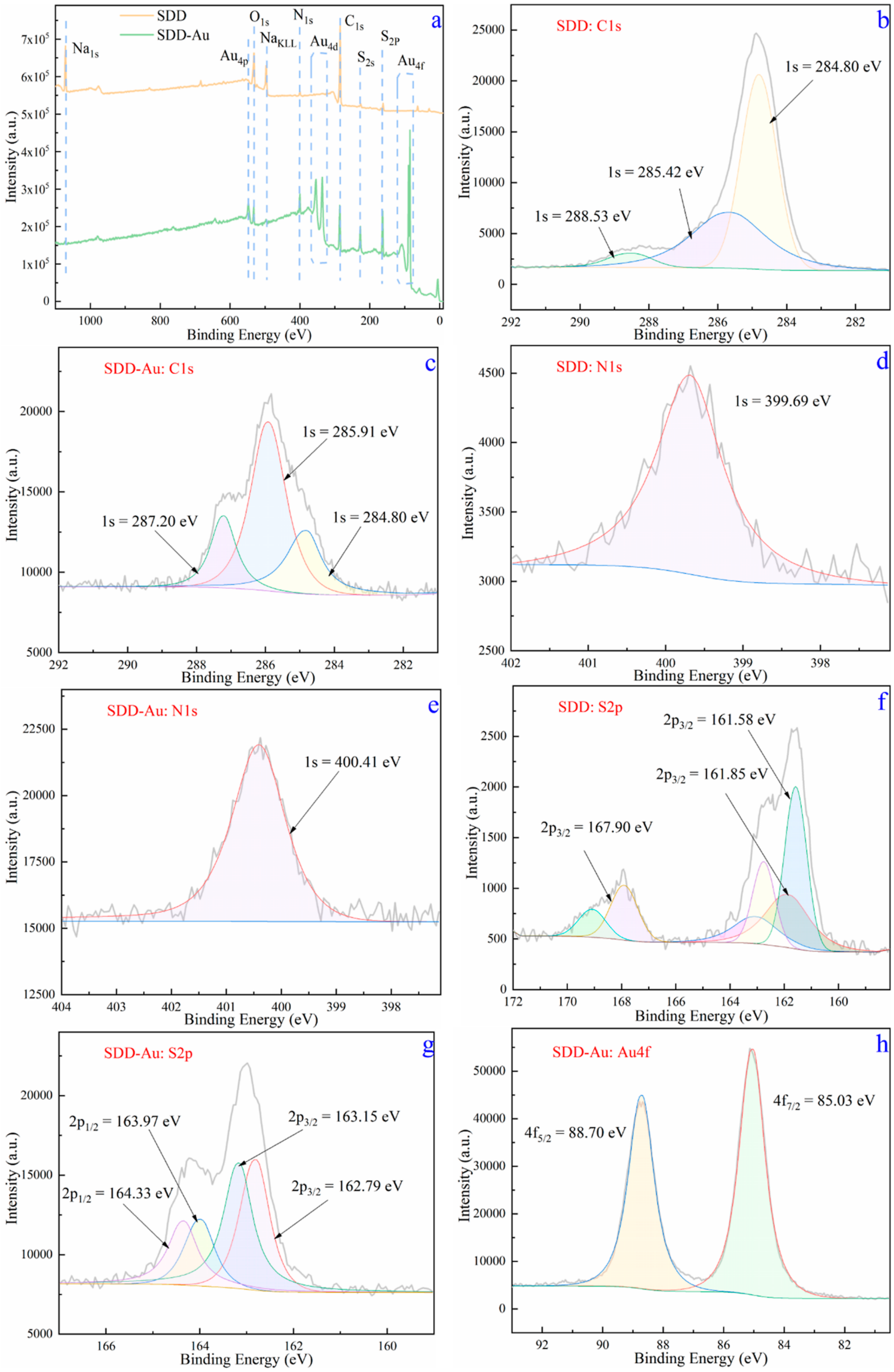

Figure 3. (a) Elemental composition and XPS spectra for (b,c) C 1s of SDD and SDD-Au, (d,e) N 1s of SDD and SDD-Au, (f,g) S 2p of SDD and SDD-Au, and (h) Au 4f of SDD-Au.

is most likely to rely on the coordination of C—S bonds in SDD and Au(I).

3.1.3. SEM-EDS Results. SEM-EDS was used to characterize the morphology and surface elemental composition of SDD and SDD-Au, where SDD-Au was obtained by reacting SDD with a thiosulfate gold leaching solution. It can be seen from Figure 4 that the surface morphology of SDD is a simple plane, which is the result of the high agglomeration of SDD molecules, and its corresponding elemental composition are C, N, O, S, and Na. Compared with SDD, obvious gold peaks can be found in the energy spectrum of SDD-Au, which indicates that SDD has successfully enriched Au(I) in solution. In addition, the surface

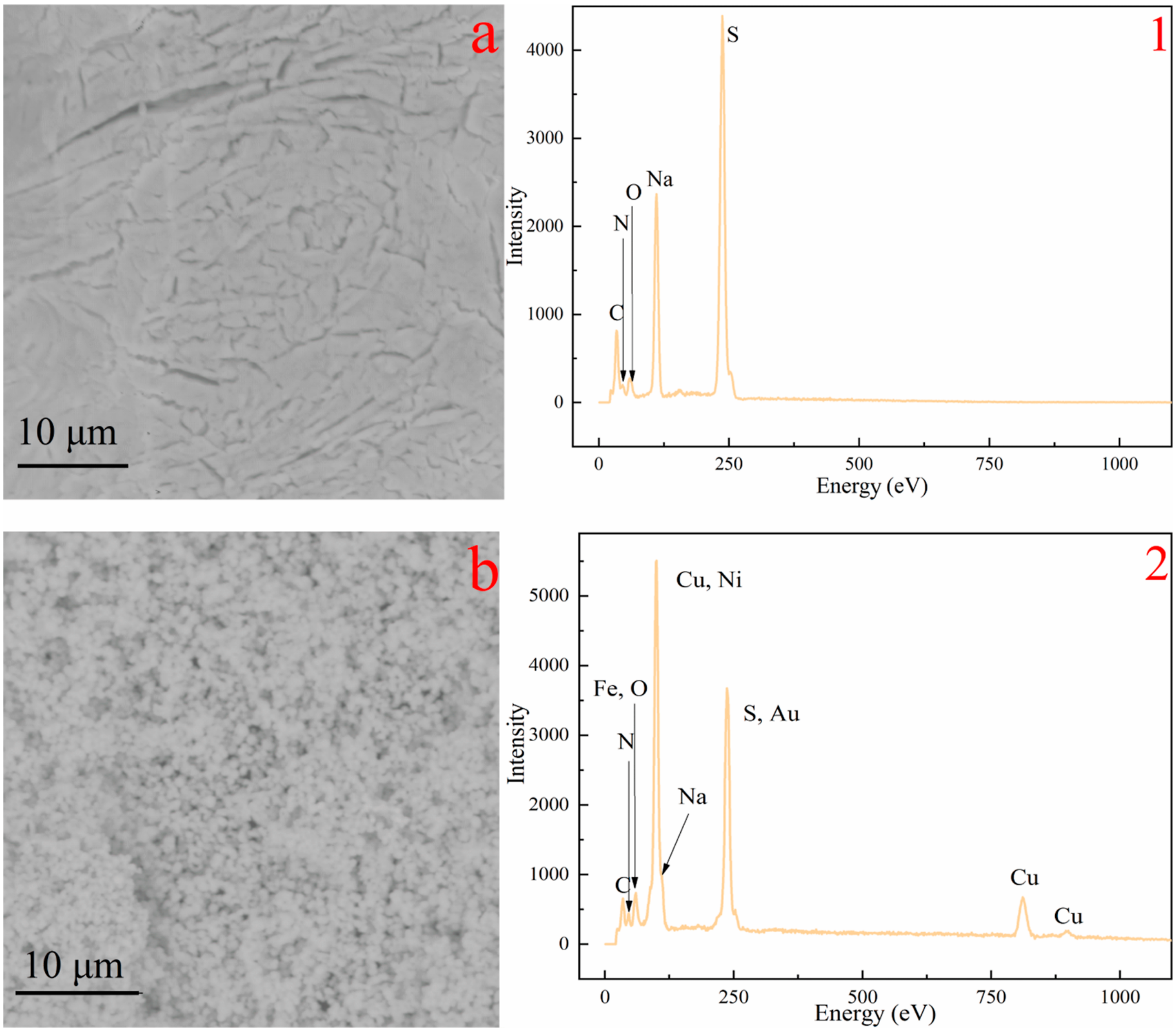

Figure 4. SEM images and corresponding EDS spectra for (a) SDD and (b) SDD-Au.

morphology of SDD-Au has changed from the original plane to a small water-insoluble particle-like substance, which indicates that one or two SDD molecules can only form a chelating complex with one Au(I) but cannot alternate with multiple Au(I) to form a flat-shaped substance.[33]

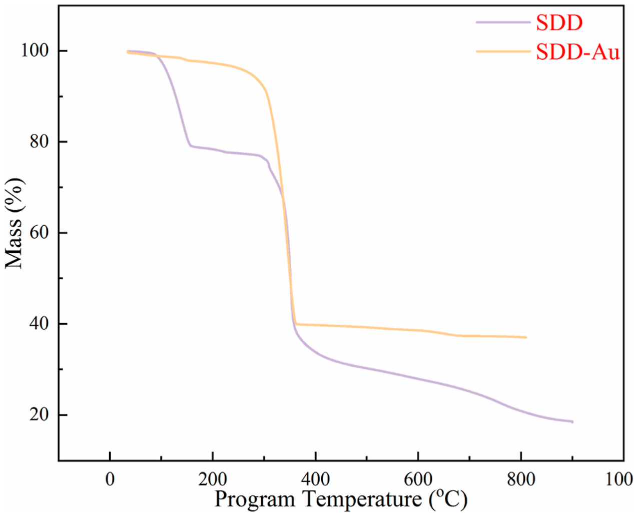

Figure 5. TGA of SDD and SDD-Au.

3.1.4. TGA Results. To determine the thermal stability of SDD and SDD-Au, the curves of the two samples were recorded in the range 35−800 °C at a 10 °C/min heating rate in N_2, as exhibited in Figure 5. It can be found that the weight loss of SDD can be clearly divided into two parts. In the range of 80−160 °C, SDD lost 20.65% of its weight rapidly due to the loss of crystal water. The weight loss in the range of 290−800 °C can be attributed to the decomposition of SDD. The decomposition of SDD can obviously be divided into two parts; in the range of 290−360 °C, the rapid weight loss of 37.12% is due to the decomposition of SDD into sulfur polymers and carbonaceous residues;[34] in the range of 360−800 °C, sulfur polymers and carbonaceous residues slowly decompose. In the curve of SDD-Au, it can be found that SDD-Au has no obvious dehydration phenomenon in the range of 80−160 °C, which may be because SDD-Au does not carry crystal water. The weight loss of SDD-Au in the range of 270−800 °C is also due to the decomposition of SDD^- in the precipitate. However, compared with SDD, the decomposition temperature of SDD-Au into polysulfides and carbonaceous residues is in the range of 270−360 °C. Furthermore, because the amount of C and S elements in SDD-Au is relatively small, the decomposition trend of polysulfide and carbonaceous residues in the range of 360−

800 °C is weaker than for SDD. Comparing the two precipitates, it can be seen that the thermal stability of SDD-Au is not as good as that of SDD, which may be due to the change of the configuration of SDD itself after the formation of a new complex.

3.2. Recovery Tests. *3.2.1. Effects of SDD Dosage on Recovering Gold.* Too much SDD will cause waste of reagents, and too little SDD will make the recovery incomplete. Therefore, the effect of the SDD dosage on recovering gold in thiosulfate leaching solution was investigated. In this study, gold was recovered from 100 mL of 17.34 mg/L gold leaching solution with different dosage of SDD at 25 °C. As can be seen from the results (Figure 6), the recovery efficiency of gold in the gold leaching solution increased with an increase in SDD dosage from 0.14 to 0.20 g; when the SDD dosage was 0.2 g, the recovery efficiency of gold in the leaching solution was >99%, and almost complete recovery of gold ions was achieved. It can be seen that for this kind of gold ore, only 2 kg of SDD is needed per ton of leaching solution to achieve complete recovery of gold ions. Compared with adsorption, solvent extraction, and metal replacement, SDD has obvious advantages in the recovery cost of Au(I) in leaching solution. Therefore, unless otherwise specified, the SDD dose will be controlled at 0.20 g in the follow-up study.

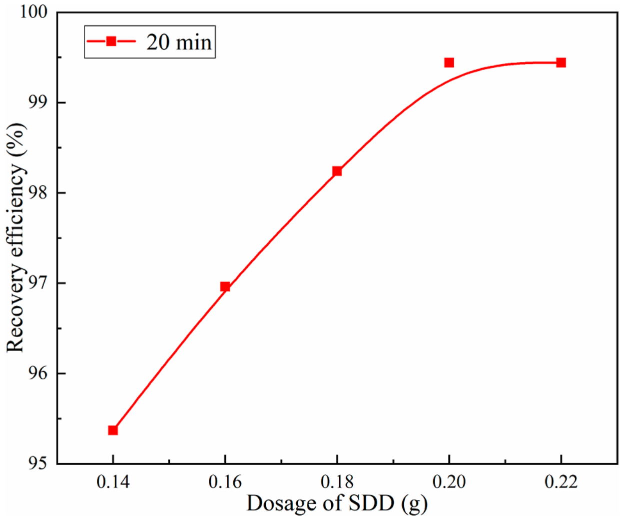

Figure 6. Effects of SDD dosage on recovering gold.

3.2.2. Effect of Recovery Time on Recovering Gold. The shortest time for SDD to reach the recovery limit of gold ions in a gold leaching solution is worth exploring. In this study, gold ions were recovered from 100 mL of 17.34 mg/L gold leaching solution at 25 °C for different times. The results are shown in Figure 7. It can be found that the recovery efficiency of gold ions was >99% after 1 min of recovery, and almost complete recovery was achieved. Compared with adsorption, solvent extraction, and metal replacement, SDD has obvious advantages in the recovery efficiency of Au(I) in leaching solution. In addition, the concentration of gold ions in the gold leaching solution did not change significantly in the following 30 min, indicating that the chelated precipitate formed by SDD and Au(I) can exist stably in solution. Therefore, unless otherwise specified, the recovery time will be controlled at 1 min in the follow-up study.

3.2.3. Effect of Recovery Temperature on Recovering Gold. Temperature is an important factor in determining the extent to which chemical reactions proceed. Here, the effect of SDD on gold recovery from a leaching solution at 25−65 °C was explored. The gold was recovered from 100 mL of 17.34 mg/L gold leaching solution, and the results are shown in Figure 8. It can be seen that the recovery efficiency values of SDD for gold after 1 min at 25 and 65 °C were 99.2 and 97.02%, respectively. The recovery of Au(I) in the gold leaching solution by SDD decreased with increasing temperature within the investigated temperature range, indicating that the process was exothermic, and higher temperature would inhibit the recovery process; the increase of temperature will make the reaction equilibrium shift to the left, which is not conducive to the recovery of Au(I) in solution by SDD^-. Overall, for the gold ore leaching solution in this experiment, the recovering capacity of SDD for Au(I) reached 7.99 kg/t, which could fully meet the needs of industrialization.

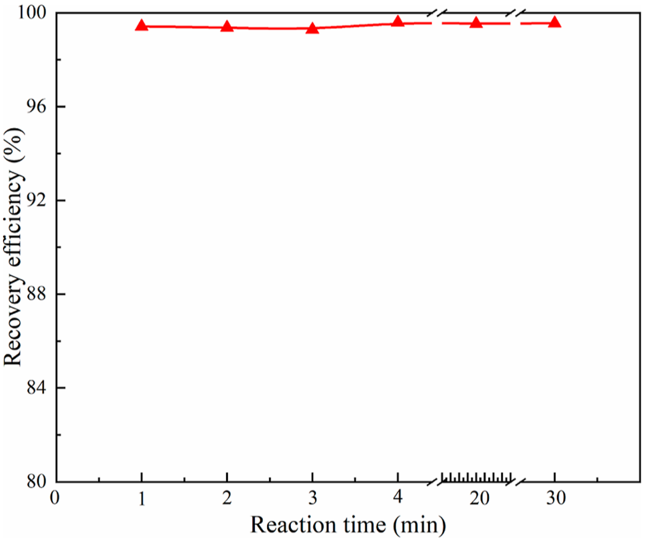

Figure 7. Effect of reaction time on recovering gold.

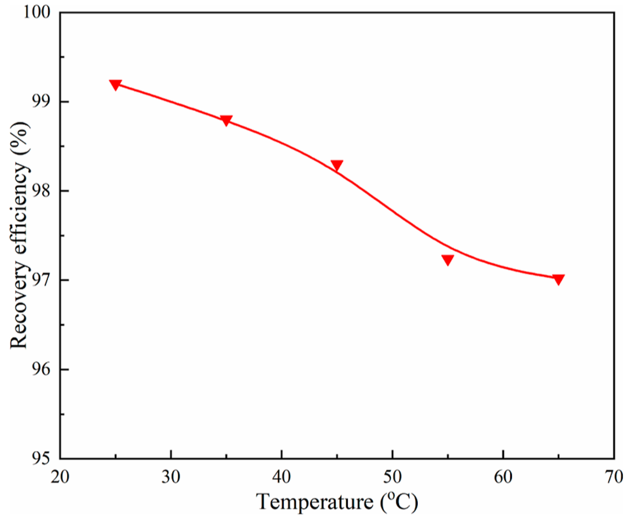

Figure 8. Effect of reaction temperature on recovering gold.

3.2.4. Effect of Different Concentrations of $Au[(S_2O_3)_2]^3$ on Recovering Gold. The recovery effect of SDD for Au(I) in low concentrations determines its application prospects. It can be seen from Figure 9 that 0.2 g of SDD can almost completely recover gold in 100 mL of 17.34 mg/L $Au[(S_2O_3)_2]^{3-}$ solution, that is, 100 mL of 1 mg/L $Au[(S_2O_3)_2]^{3-}$ solution requires

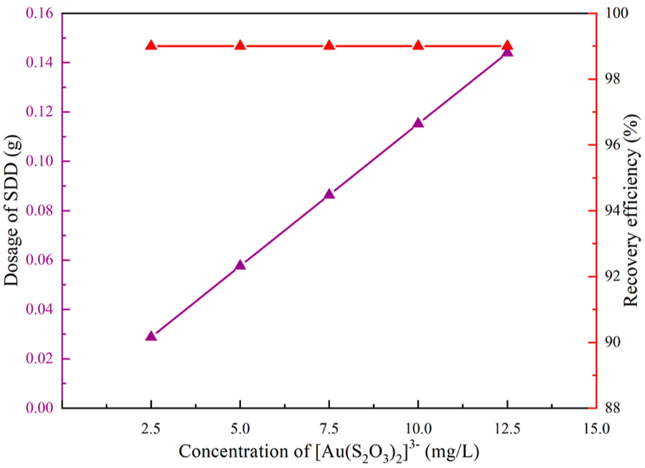

Figure 9. Effect of different concentrations of $Au[(S_2O_3)_2]^{3-}$ on recovering gold.

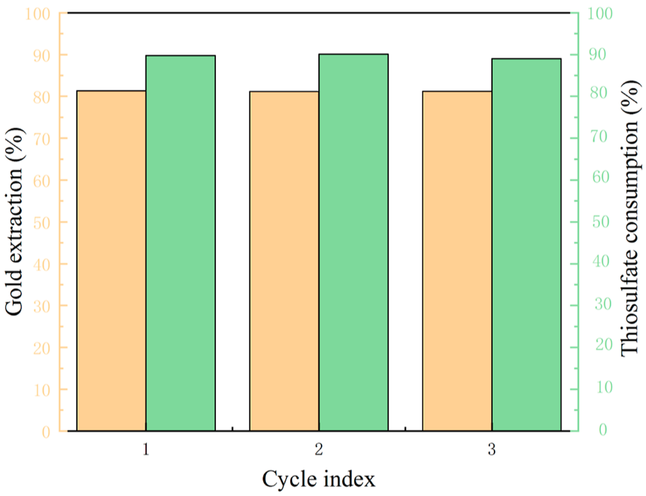

Figure 10. Effect of gold leaching solution reuse on leaching gold.

0.0115 mg of SDD. According to this ratio, the recovery efficiency of SDD for Au(I) under different concentrations was explored. The $Au[(S_2O_3)_2]^{3-}$ concentrations were 2.5, 5, 7.5, 10, and 12.5 mg/L, and the corresponding SDD dosages were 0.0288, 0.0575, 0.0862, 0.1150, and 0.1437 g, respectively. The results are listed in Figure 9. It could be found that the recovery of gold ions could be almost achieved by adding SDD dosage proportionally to $Au[(S_2O_3)_2]^{3-}$ solution at different concentrations, which indicates that SDD has a good recovery effect for Au(I) in both high and low concentrations; this is another advantage compared to adsorption, solvent extraction, and metal replacement.

3.2.5. Effect of Leaching Solution Recycling on Leaching Gold. Recycling of the leaching solution is crucial in the hydrometallurgical process. The effect of recycling of the aqueous solution after SDD recovering Au(I) on leaching gold was explored. First, after measuring the $S_2O_3{}^{2-}$ concentration in the gold leaching solution, SDD was added to the gold leaching solution according to the guideline that 1 mg/L $Au[(S_2O_3)_2]^{3-}$ solution requires 0.0115 mg chelating agent. Next, 5 mL of Cu−NH_3 solution was added to the gold leaching solution to ensure that there was no residual SDD. The concentrations of Cu^{2+} and ammonia in the aqueous solution obtained after filtration were measured, then Cu^{2+} and ammonia were added in the solution to ensure that the concentration of the Cu−NH_3 complex was 5 mmol/L, and the mol ratio of cupric ion and ammonia was 1:80. Finally, after the concentration of sodium thiosulfate was supplemented to 0.1 mol/L, the mixed solution was mixed with gold ores, and leaching of gold was started according to the method described in Section 2.2.3. The aqueous solution was treated according to the steps described above before each repeated solution-recycling experiment. The results after recycling of the gold leaching solution three times are shown in Figure 10. It can be seen from Figure 10 that the recycling of gold leaching solution will not affect the leaching of gold ores, and its leaching rate was basically maintained at 81%. In addition, the consumption of thiosulfate was not affected by the recycling of the gold leaching solution, and the consumption of thiosulfate was maintained at 89% each time during the recycling. Therefore, the gold leaching solution after recovering gold by SDD can be recycled without significant influence on the gold leaching effect and reagent consumption.

3.2.6. Recovery Mechanism. To investigate the composition ratio between SDD^- and Au(I) in SDD-Au, a certain amount of SDD was added to pure $Au[(S_2O_3)_2]^{3-}$ solution to obtain SDD-Au; with an accurately weighed 0.0108 g of SDD-Au dissolved in aqua regia with a volume ratio of 1:1, the gold ion concentration in the solution was determined by AAS, and it was calculated that the mass of gold ions was 4.985 mg, that is, 0.0253 mmol. If the composition ratio of SDD^- and Au(I) in the precipitate is 1:1, then the amount of SDD^- is 0.0484 mmol. Obviously, this kind of composition is impossible. If the composition ratio of SDD^- and Au(I) in the precipitate is 2:1, then its composition is $[(SDD^-)\text{-}Au^+\text{-}(SDD^-)]^-$ or $[(SDD^-)Au^+(SDD^-)]^-M^+$; the cations present in the solution are H^+ and Na^+. When its composition is the first case, the amount of $2SDD^-$ is 0.0242 mmol, and its composition ratio to Au(I) is 0.96:1. In the second composition case, when the cation is H^+, the amount of $2SDD^-$ is 0.0241 mmol, that is, the composition ratio of $2SDD^-$ to Au(I) is 0.95:1; when the cation is Na^+, the amount of $2SDD^-$ is 0.0241 mmol, that is, the composition ratio of $2SDD^-$ to Au(I) is 0.87:1. Obviously, excluding the error factor, the composition ratio of SDD^- and Au in SDD-Au being 2:1 is reasonable. Therefore, the composition ratio of SDD^- to Au(I) in SDD-Au was taken as 2:1.

Quantum chemical calculations were used to further confirm the action mechanism and composition ratio of SDD^- to Au(I) in SDD-Au. The optimized geometries of the SDD, SDD^-, $(SDD^-)\text{-}Au^+$, $(2SDD^-)\text{-}Au^+$, and $Au[(S_2O_3)_2]^{3-}$ complexes are shown in Figure 11, and the relevant partial energies is listed in Table 2. It can be seen from Table 2 that the binding energies of $(SDD^-)\text{-}Au^+$ and $(2SDD^-)\text{-}Au^+$ are −833.50 and −1060.73 kJ/mol, respectively, which indicates that both structures are possible. However, the binding energy of $(2SDD^-)\text{-}Au^+$ is larger than that of $(SDD^-)\text{-}Au^+$, indicating that the presence of the former is more stable than that of the latter. Obviously, the calculated results are consistent with the conclusion obtained through experiments that the composition ratio between SDD^- and Au(I) is 2:1. Therefore, it can be confirmed that the composition ratio between SDD^- and Au in the chelating complex SDD-Au is 2:1.

The calculator molecule parameters are listed in Table 3. In SDD, the bond lengths of C−S and C═S in SDD are both 1.74 Å, and the bond length of C−N is 1.35 Å. Obviously, the coexistence of C−S and C═S increases the degree of

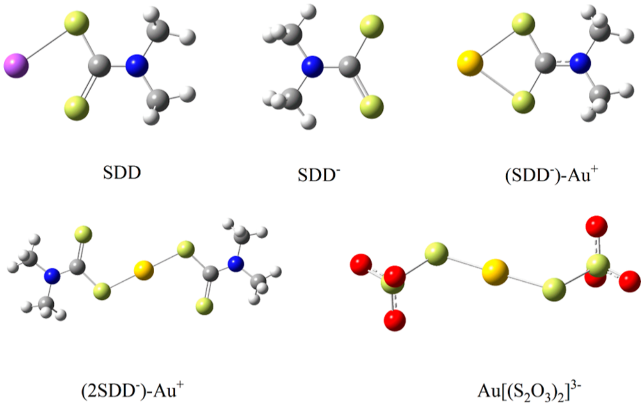

Figure 11. Optimized geometries of SDD, SDD$^-$, (SDD$^-$)-Au$^+$, (2SDD$^-$)-Au$^+$, and [Au$(S_2O_3)_2$]$^{3-}$.

Table 2. Energies of Au(I), (SDD$^-$)-Au$^+$, (2SDD$^-$)-Au$^+$, and SDD$^-$

ions	energies (kJ/mol)
Au(I)	-3.55×10^5
(SDD$^-$)-Au$^+$	-2.90×10^6
(2SDD$^-$)-Au$^+$	-5.44×10^6
SDD$^-$	-2.54×10^6
E [(SDD$^-$)-Au$^+$]−E (SDD$^-$)−E (Au(I))	−833.50
E [(2SDD$^-$)-Au$^+$]−E (2SDD$^-$)−E (Au(I))	−1060.73

Table 3. Calculated Molecular Parameters

ions	symbol	bond (Å)
SDD	C−S	1.74
	C═S	1.74
	C−N	1.35
SDD$^-$	C−S	1.72
	C═S	1.72
	C−N	1.39
(2SDD$^-$)-Au$^+$	C−S	1.76
	C═S	1.69
	C−N	1.38
	S−Au	2.38
[Au$(S_2O_3)_2$]$^{3-}$	S−Au	2.41

delocalization, resulting in an average of the single and double bond lengths. In SDD$^-$, it can be found that the bond lengths of C−S and C═S in SDD$^-$ are shortened from the original 1.74 to 1.72 Å, while the C−N bond length is increased from 1.35 to 1.39 Å. Apparently, SDD$^-$ and cationic reactions result in changes in the chemical environment of C−S, C═S, and C−N. In (2SDD$^-$)-Au$^+$, the formation of coordination bonds between C−S and Au enhances the C═S bond in the ligand, and the bond length was reduced from 1.72 to 1.69 Å, while the C−S single bond was increased from 1.72 to 1.76 Å. Obviously, the formation of (2SDD$^-$)-Au$^+$ reduces the degree of delocalization. The C−N bond length here is shortened from the original length of 1.39 to 1.38 Å, indicating that the C−N bond in (2SDD$^-$)-Au$^+$ has a tendency to form a double bond. In addition, from the optimized geometry of (2SDD$^-$)-Au$^+$, it can be seen that the optimal structure is that S in C−S is coordinated with Au(I), and C═S is not transformed into the C−S bond to directly participate in the coordination in this process, which is consistent with the conclusions of FT-IR and XPS. It can also be found from Table 3 that the S−Au bond length in (2SDD$^-$)-Au$^+$ is 2.38 Å and the S−Au bond length in Au[$(S_2O_3)_2$]$^{3-}$ is 2.4 Å, indicating that the interaction intensity between S and Au in the former is stronger than that in the latter, which is also the reason why SDD$^-$ can form a chelating complex with Au in Au[$(S_2O_3)_2$]$^{3-}$.

The charge distributions of SDD$^-$ and (2SDD$^-$)-Au$^+$ were analyzed by Frontier orbital theory calculations and natural bond orbital (NBO) analysis. The highest occupied molecular orbitals (HOMOs) and lowest unoccupied molecular orbitals (LUMOs) of SDD$^-$ and (2SDD$^-$)-Au$^+$ are shown in Figure 12.

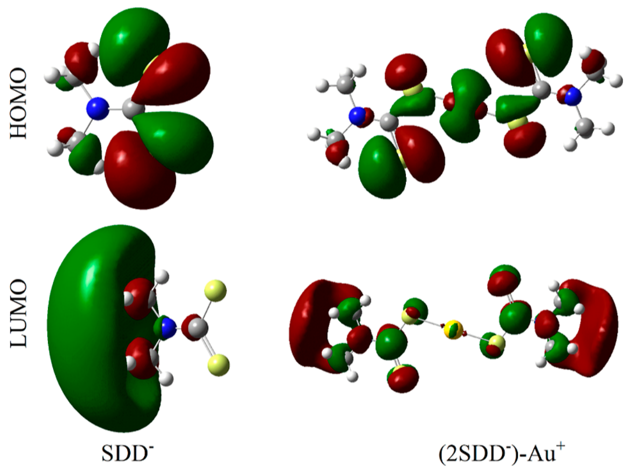

Figure 12. Frontier molecular orbitals of SDD$^-$ before and after the coordination process.

The HOMO of SDD$^-$ is mainly located on the S atom on the C−S and C═S bonds, while the LUMO is mainly located on the two methyl groups at the other end. However, compared to SDD, the HOMO of (2SDD$^-$)-Au$^+$ changed greatly, and a large part of the HOMO of the S atom on the C−S bond was transferred to the Au atom. Obviously, the formation of (2SDD$^-$)-Au$^+$ mainly depended on the interaction between the C−S bonds of SDD and Au(I). Furthermore, it can be found that the LUMOs of (2SDD$^-$)-Au$^+$ also changed significantly. The changes in HOMOs and LUMOs before and after SDD$^-$ coordination indicated that the charge was transferred from the ligand to Au(I) during the formation of the chelating complex, resulting in a change in the orbital properties. Table 4 lists the electron configurations of Au(I) and partial NBO charges. The net charge of the Au ion in (2SDD$^-$)-Au$^+$ is 0.234, while the charge of conventional Au(I) is 1, indicating that the charge on SDD$^-$ is transferred to Au(I) during the formation of the chelating complex. The electronic configuration of Au(I) changes from $5d^{10}$ to $6S^{0.83}5d^{9.78}6p^{0.15}$, indicating that the charge is mainly transferred from SDD- to the empty 6s orbital of Au(I).

Table 4. NBO Partial Charges on the Fragments and Electron Configurations of Au(I)

complex	NBO partial charges		Au(I) electron configuration
	ligand	Au(I)	
(2SDD$^-$)-Au$^+$	−0.234	0.234	$6S^{0.83}5d^{9.78}6p^{0.15}$

The interaction between the C−S bond and Au(I) was confirmed by FT-IR and XPS. In addition, the composition ratios between SDD- and Au(I) were actually confirmed by stoichiometry, and the feasibility of the conclusion was theoretically verified by DFT calculation. Therefore, it can be determined that the formation of SDD-Au mainly depends on the exchange of ligands between SDD^- and $[Au(S_2O_3)_2]^{3-}$ in solution, and the composition ratio of SDD and Au is 2:1. When $[Au(S_2O_3)_2]^{3-}$ comes in contact with C−S, the sulfur atom contributes electrons to Au(I), which in turn provides the oxygen atom with empty orbitals. The mechanism of SDD recovering Au(I) can be expressed as follows

$$Au(S_2O_3)_2{}^{3-} \rightleftharpoons Au^+ + 2S_2O_3{}^{2-} \tag{4}$$

$$(CH_3)_2NCSSNa \rightleftharpoons (CH_3)_2NCSS^- + Na^+ \tag{5}$$

$$\begin{aligned} &Au(S_2O_3)_2{}^{3-} + 2(CH_3)_2NCSS^- \\ &\quad \rightleftharpoons [((CH_3)_2NCSS)_2Au]^- + 2S_2O_3{}^{2-} \end{aligned} \tag{6}$$

4. CONCLUSIONS

In this study, in view of the deficiencies of the existing recovery methods, SDD was used as a chelating precipitant to achieve efficient recovery of gold ions in a thiosulfate gold leaching solution and recycling of the lixiviant and ammonia. Moreover, the adsorption mechanism of Au(I) on VE-TPPO was investigated by DFT calculations and various characterization methods. The results of this study are summarized as follows:

1. Outstanding gold recovery effect was achieved with a dosage of SDD of approximately 0.2 g, the temperature of approximately 25 °C, and the time of approximately 1 min for a solution containing 17.34 mg/L gold. The recovery efficiency of Au(I) by SDD increased with the decrease of solution temperature, and the recovering capacity was 7.99 kg/t at a gold concentration of 17.34 mg/L at 25 °C.
2. After two cycle experiments on ammonia and the lixiviant in the gold leaching solution, it was found that recycling of ammonia and the lixiviant will not significantly impact the gold leaching effect and the consumption of thiosulfate, and their values were basically maintained at 81 and 89%, respectively, demonstrating that this method can well realize the recycling of the leaching solution.
3. The gold recovery mechanism was confirmed to involve ligand exchange between SDD and $[Au(S_2O_3)_2]^{3-}$. The empty 6s orbital of Au in SDD-Au accepts electrons from SDD^-, and the composition ratio of SDD^- and Au in SDD-Au is 2:1.

Clearly, the recovery method proposed in this study can continue to be explored as a new idea, which is ideal for industrial production.

■ AUTHOR INFORMATION

Corresponding Author

Xianzhi Hu − *Faculty of Science, Kunming University of Science and Technology, Kunming 650500, China;* orcid.org/0000-0003-2558-5693; Phone: +8613508808699; Email: xianzhihu2@sina.com

Authors

Peng Yang − *Faculty of Land Resource Engineering, Kunming University of Science and Technology, Kunming 650093, China; Faculty of Science, Kunming University of Science and Technology, Kunming 650500, China*

Xinrong Li − *Faculty of Land Resource Engineering, Kunming University of Science and Technology, Kunming 650093, China*

Shuliang Chen − *Faculty of Land Resource Engineering, Kunming University of Science and Technology, Kunming 650093, China*

Futing Zi − *Faculty of Science, Kunming University of Science and Technology, Kunming 650500, China*

Complete contact information is available at: https://pubs.acs.org/10.1021/acsomega.4c01941

Notes

The authors declare no competing financial interest.

■ ACKNOWLEDGMENTS

This paper was financially supported by the Natural Science Foundation of China (51674128; 21764008). The authors sincerely express gratitude to Professor Guocai Tian of Kunming University of Science and Technology for his help and support.

■ REFERENCES

(1) Moussavi, G.; Pourakbar, M.; Aghayani, E.; Mahdavianpour, M. Investigating the aerated VUV/PS process simultaneously generating hydroxyl and sulfate radicals for the oxidation of cyanide in aqueous solution and industrial wastewater. *Chem. Eng. J.* **2018**, *350*, 673−680.

(2) Mahandra, H.; Faraji, F.; Ghahreman, A. Novel Extraction Process for Gold Recovery from Thiosulfate Solution Using Phosphonium Ionic Liquids. *ACS Sustainable Chem. Eng.* **2021**, *9* (24), 8179−8185.

(3) Wang, C.; Chen, S.; Chen, Y.; Zi, F.; Hu, X.; Qin, X.; Zhang, Y.; Yang, P.; He, Y.; He, P.; et al. Modification of activated carbon by chemical vapour deposition through thermal decomposition of thiourea for enhanced adsorption of gold thiosulfate complex. *Sep. Purif. Technol.* **2020**, *241*, 116632.

(4) Chen, Y. L.; Zi, F. T.; Hu, X. Z.; Yang, P.; Ma, Y. P.; Cheng, H. L.; Wang, Q.; Qin, X. C.; Liu, Y.; Chen, S. L.; et al. The use of new modified activated carbon in thiosulfate solution: A green gold recovery technology. *Sep. Purif. Technol.* **2020**, *230*, 115834.

(5) Zhao, L.; Hu, X. Z.; Zi, F. T.; Chen, S. L.; Cheng, H. L.; Yang, P.; Zhang, Y.; Chen, Y. L.; Jiang, Y. S.; Li, X. R.; et al. Development of Stable, Efficient, and Recyclable Amine-Containing Microspheres for Gold(I) Thiosulfate Complex Recovery. *ACS Sustainable Chem. Eng.* **2022**, *10*, 14624−14635.

(6) Chen, S.; Zi, F.; Hu, X.; Chen, Y.; Yang, P.; Wang, Q.; Qin, X.; Cheng, H.; Liu, Y.; He, Y.; et al. Interfacial properties of mercaptopropyl-functionalised silica gel and its adsorption performance in the recovery of gold(I) thiosulfate complex. *Chem. Eng. J.* **2020**, *393*, 124547.

(7) Chen, Y.; Zi, F.; Hu, X.; Lin, Y.; Du, H.; Hu, J.; Yang, P.; Zhang, Y.; Yang, B. The first effective utilization of activated carbon in gold thiosulfate system: A more eco-friendly, easier method for gold recovery and material regeneration. *Miner. Eng.* **2020**, *155*, 106441.

(8) Chen, Y.; Zi, F.; Hu, X.; Yu, H.; Nie, Y.; Yang, P.; Cheng, H.; Wang, Q.; Qin, X.; Chen, S.; et al. Grafting of organic sulfur-containing functional groups on activated carbon for gold(I) adsorption from thiosulfate solution. *Hydrometallurgy* **2019**, *185*, 102−110.

(9) Li, X. R.; Chen, S. L.; Hu, X. Z.; Zi, F. T. Efficient and Selective Recovery of Gold from Thiosulfate Leaching Solution Using Functionalized *β*-Cyclodextrins Synthesized by a Steric Hindrance Strategy. *Adv. Funct. Mater.* **2024**, *34*..

(10) Kejun, L.; Yen, W. T.; Shibayama, A.; Miyazaki, T.; Fujita, T. J. Gold extraction from thiosulfate solution using trioctylmethylammonium chloride. *Hydrometallurgy* **2004**, *73* (1−2), 41−53.

(11) Arima, H.; Fujita, T.; Yen, W. Gold Cementation from Ammonium Thiosulfate Solution by Zinc, Copper and Aluminium Powders. *Mater. Trans.* **2002**, *43* (3), 485−493.

(12) Yu, H.; Zi, F.; Hu, X.; Nie, Y.; Xiang, P.; Xu, J.; Chi, H. Adsorption of the gold-thiosulfate complex ion onto cupric ferrocyanide (CuFC)-impregnated activated carbon in aqueous solutions. *Hydrometallurgy* **2015**, *154*, 111−117.

(13) Zeng, S.; Jia, F.; Yang, B.; Song, S. In-situ reduction of gold thiosulfate complex on molybdenum disulfide nanosheets for a highly-efficient recovery of gold from thiosulfate solutions. *Hydrometallurgy* **2020**, *195*, 105369.

(14) Sun, K.; Mao, S.; Zhan, W.; Liu, C.; Jia, F.; Song, S. In-situ reduction of Au(S2O3)23 for efficient recovery of gold with magnetically separable shell-core structured MoS2@Fe3O4 composite. *Hydrometallurgy* **2020**, *198* (3), 105514.

(15) Liu, W.; Wei, D.; Mi, J.; Shen, Y.; Cui, B.; Han, C. Immobilization of Cu(II) and Zn(II) in simulated polluted soil using sulfurizing agent. *Chem. Eng. J.* **2015**, *277*, 312−317.

(16) Li, X. R.; Zhao, L.; Chen, S. L.; Lin, Y.; Hu, X. Z.; Zi, F. T. Highly efficient and selective extraction of Au(I) from thiosulfate gold-leaching solution using diphenylphosphine. *J. Environ. Chem. Eng.* **2024**, *12* (1), 111750.

(17) Kara, I.; Akar, S. T.; Akar, T.; Ozcan, A. Dithiocarbamated Symphoricarpus albus as a potential biosorbent for a reactive dye. *Chem. Eng. J.* **2012**, *211*−*212*, 442−452.

(18) Singh, N.; Bhattacharya, S. Synthesis and characterization of some triorgano, diorgano, monoorganotin and a triorganolead heteroaromatic dithiocarbamate complexes. *J. Organomet. Chem.* **2012**, *700*, 69−77.

(19) Zhen, H. B.; Xu, Q.; Hu, Y. Y.; Cheng, J. H. Characteristics of heavy metals capturing agent dithiocarbamate (DTC) for treatment of ethylene diamine tetraacetic acid-Cu (EDTA-Cu) contaminated wastewater. *Chem. Eng. J.* **2012**, *209* (none), 547−557.

(20) Ifthikar, J.; Chen, Z.; Chen, Z.; Jawad, A. A Self-Gating Proton-coupled Electron Transfer Reduction of Hexavalent Chromium by Core-shell SBA-Dithiocarbamate Chitosan Composite. *J. Hazard. Mater.* **2020**, *384*, 121257.

(21) Sarwar, M.; Ahmad, S.; Ahmad, S.; Ali, S.; Awan, S. A. Copper(II) complexes of pyrrolidine dithiocarbamate. *Transition Met. Chem.* **2007**, *32* (2), 199−203.

(22) Nakakubo, K.; Hasegawa, H.; Ito, M.; Yamazaki, K.; Miyaguchi, M.; Biswas, F. B.; Ikai, T.; Maeda, K. Dithiocarbamate-modified cellulose resins: A novel adsorbent for selective removal of arsenite from aqueous media. *J. Hazard. Mater.* **2019**, *380*, 120816.

(23) Huang, X.; Cao, X.; Wang, W.; Zhong, H.; Cao, Z. F. Investigation of removal of Ag(I) from aqueous solution by a novel chelating resin containing acyl and thiourea groups. *J. Dispersion Sci. Technol.* **2019**, *40* (4), 477−486.

(24) Fbba, E.; Immr, B.; Kn, A.; Ky, A.; Mea, C.; Knc, A.; Asm, D.; Tt, D.; Tn, D.; Km, D. Selective recovery of silver and palladium from acidic waste solutions using dithiocarbamate-functionalized cellulose. *Chem. Eng. J.* **2020**, *407*, 127225.

(25) Descostes, M.; Mercier, F.; Thromat, N.; Beaucaire, C.; Gautier-Soyer, M. Use of XPS in the determination of chemical environment and oxidation state of iron and sulfur samples: constitution of a data basis in binding energies for Fe and S reference compounds and applications to the evidence of surface species of an oxidized pyrite in a carbonate medium. *Appl. Surf. Sci.* **2000**, *165* (4), 288−302.

(26) Bourg, M. C.; Badia, A.; Lennox, R. B. GoldSulfur Bonding in 2D and 3D Self-Assembled Monolayers: XPS Characterization. *J. Phys. Chem. B* **2000**, *104* (28), 6562−6567.

(27) Ashton, M. R.; Jones, T. S.; Richardson, N. V.; Mack, R. G.; Unertl, W. N. The chemisorption of polyimide precursors and related molecules on metal surfaces. *J. Electron. Spectrosc.* **1990**, *54*−*55* (none), 1133−1142.

(28) Peeling, J.; Hruska, F. E.; Mckinnon, D. M.; Chauhan, M. S.; Mcintyre, N. S. ESCA studies of the uracil base. The effect of methylation, thionation, and ionization on charge distribution. *Can. J. Chem.* **1978**, *56* (18), 2405−2411.

(29) Wu, P. X.; Tang, Y. N.; Wang, W. M.; Zhu, N. W.; Li, P.; Wu, J. H.; Dang, Z.; Wang, X. Effect of dissolved organic matter from Guangzhou landfill leachate on sorption of phenanthrene by Montmorillonite. *J. Colloid Interface Sci.* **2011**, *361* (2), 618−627.

(30) Achilleos, A. A.; Gahan, L. R.; Hambley, T. W.; Healy, P. C.; Weedon, D. M. Structural and x-ray photoelectron spectroscopic properties of hydrophobic cobalt(III) 'Cage' complexes with dithiocarbamate anions. *Inorg. Chim. Acta* **1989**, *157* (2), 209−214.

(31) Hartung, J.; Weber, G.; Beyer, L.; Szargan, R.; Kreutzmann, J. Schwermetallchelate von α-Cyano-β-amino-dithioacrylsäureestern. *Z. Anorg. Allg. Chem.* **1986**, *543* (12), 186−191.

(32) Cheng, R.; Ou, S.; Li, Y.; Xiang, B. Kinetics and molecular mechanism of chromate uptake by dithiocarbamate functionalized starch. *J. Appl. Polym. Sci.* **2012**, *124*, 2930−2936.

(33) Zhang, M.; Guo, M.; Zhang, B.; Li, F.; Wang, H.; Zhang, H. Stabilization of heavy metals in MSWI fly ash with a novel dithiocarboxylate-functionalized polyaminoamide dendrimer. *Waste Manage.* **2020**, *105*, 289−298.

(34) Ramos, L. A.; Cavalheiro, É. T. G.; Chierice, G. O. Preparation, characterization and thermal decomposition of ammonium salts of dithiocarbamic acids. *J. Therm. Anal. Calorim.* **2005**, *79* (2), 349−353.

https://doi.org/10.1021/acsomega.4c01941
ACS Omega 2024, 9, 20547−20556